Mechanism and Kinetics of Photoisomerization of a Cyclic Disulfide, *trans*-4,5-Dihydroxy-1,2-dithiacyclohexane

Lorena B. Barrón,[†] Kenneth C. Waterman,[‡] Piotr Filipiak,[§] Gordon L. Hug,[§] Thomas Nauser,[†] and Christian Schöneich*[,†]

Department of Pharmaceutical Chemistry, 2095 Constant Avenue, University of Kansas, Lawrence, Kansas 66047, Pfizer Global Research and Development, Eastern Point Road, Groton, Connecticut 06340, and Radiation Laboratory, University of Notre Dame, Notre Dame, Indiana 46556

Received: November 25, 2003; In Final Form: January 30, 2004

The photolysis of *trans*-4,5-dihydroxy-1,2-dithiacyclohexane in aqueous and CH_2Cl_2 solution yields two isomers of 2,3-dihydroxy-1-mercaptotetrahydrothiophene, characterized by ^1H and ^{13}C NMR and negative ion electrospray mass spectrometry. Product formation in water is independent of the presence of oxygen and the concentration of *trans*-4,5-dihydroxy-1,2-dithia-cyclohexane and involves *intra*molecular 1,5-H-transfer, followed by cyclization through thiophilic or nucleophilic addition, or 1,2-H-transfer, followed by cyclization through the recombination of a sulfur- and a carbon-centered radical. In contrast, the quantum yields for reaction in CH_2Cl_2 solutions are dependent on both oxygen concentration and on the concentration of *trans*-4,5-dihydroxy-1,2-dithiacyclohexane. The latter results are consistent with an *inter*molecular H-transfer between an initial dithiyl diradical and *trans*-4,5-dihydroxy-1,2-dithia-cyclohexane. Time-resolved laser flash photolysis studies indicate rapid product formation on the submicrosecond time scale and support the intermediacy of α-mercaptoalkyl radicals.

Introduction

The disulfide bond, R−S−S−R, represents an important structural element in proteins.[1] Moreover, disulfide entities are part of polysulfide systems, which are found in an ever-increasing list of natural products with promising therapeutic properties.[2−5] Aliphatic disulfides generally show absorption spectra with $\lambda_{max} < 300$ nm, depending on the dihedral angle of the C−S−S−C system.[6] Depending on the nature of R, the exposure of aliphatic disulfides to UV light results in homolytic cleavage of either the S−S bond (reaction 1), generating a pair of thiyl radicals (RS•), or the C−S bond (reaction 2), generating a carbon-centered radical and a perthiyl radical (RSS•).[7,8]

$$RSSR \rightarrow 2\ RS^{\bullet} \quad (1)$$

$$RSSR \rightarrow RSS^{\bullet} + R^{\bullet} \quad (2)$$

These geminate pairs of product radicals are generated within a solvent cage. They enter various reaction channels, depending on the electronic configuration of the radical pair in the solvent cage (viz., singlet vs triplet), the rate of escape from the solvent cage, and the presence of oxygen and additional electron or hydrogen donors. For example, an important reaction of thiyl radicals is the reversible addition of oxygen, yielding thiylperoxyl radicals (RSOO•) (reaction 3) which can subsequently rearrange irreversibly to sulfonyl radicals (reaction 4) (for 2-mercaptoethanol in aqueous solution, $k_3 = 2.2 \times 10^9$ M^{-1} s^{-1}, $k_{-3} = 6.2 \times 10^5$ s^{-1}, and $k_4 = 2 \times 10^3$ s^{-1}).[9] These reactions are in competition with various other potential reaction pathways such as disproportionation, intra- and intermolecular hydrogen transfer, and radical−radical recombination.

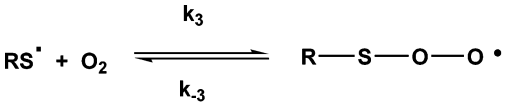

(3)

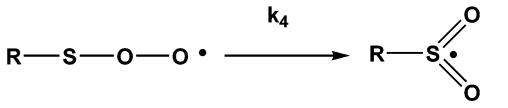

(4)

A pair of thiyl radicals generated from a high molecular weight protein disulfide should remain longer in a solvent cage than an analogous pair of thiyl radicals from compounds of lower molecular weight. In proteins, the separation of the radical pair will depend on the stability of the secondary and tertiary structure, the kinetics of unfolding, the conformational dynamics of the specific protein domain surrounding the radical pair, and the diffusion coefficient(s) of the polypeptide chain(s). Hence, under such conditions the relative efficiencies of the different reaction channels may be significantly different than with low molecular weight disulfides, though no systematic studies of these reactions in proteins have been undertaken.

Two objectives motivated the present study. First, we believe that the photolysis of a cyclic disulfide would mimic the situation of a thiyl radical pair within a protein, with restricted mobility. Second, we wanted to establish the photochemical reactions of a cyclic disulfide, which could potentially be used as an initiator for the controlled photochemical initiation of radical reactions in the solid state (solid-state hydrogen-transfer reactions are of fundamental importance[10−13] and may be initiated through the controlled generation of thiyl radicals).

* Corresponding author. Phone: (785) 864-4880. Fax: (785) 864-5736. E-mail: schoneic@ukans.edu.
[†] University of Kansas.
[‡] Pfizer Global Research and Development.
[§] University of Notre Dame.

10.1021/jp037598s CCC: $27.50
Published on Web 03/03/2004

SCHEME 1

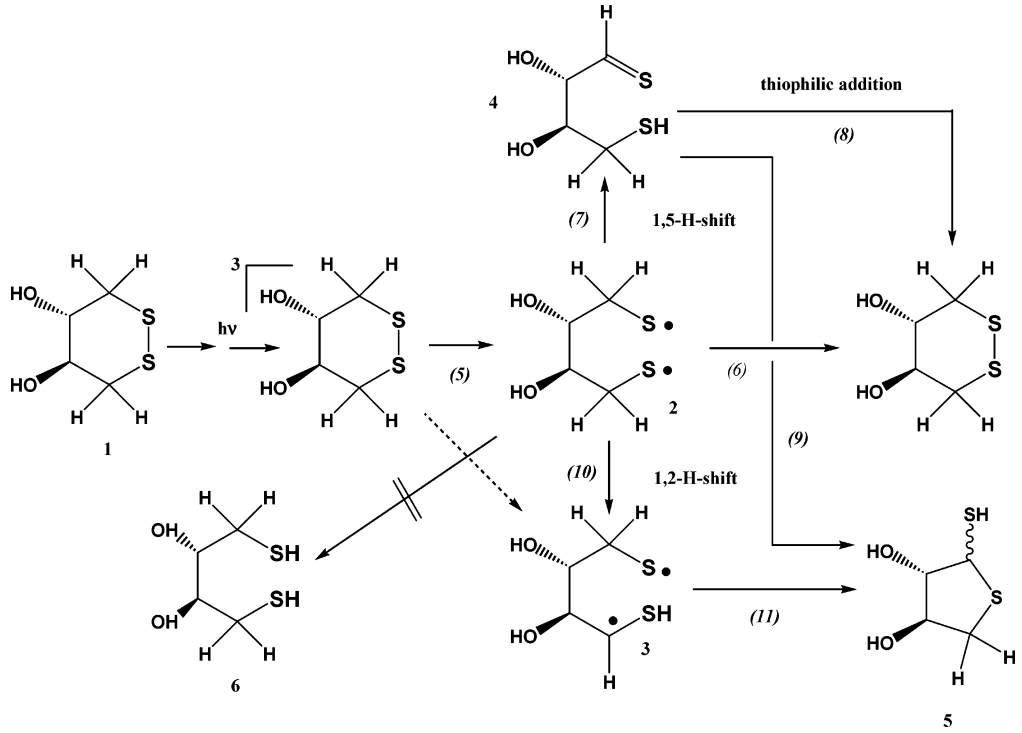

Therefore, we selected to study the photolysis and mechanisms of product formation for the cyclic organic disulfide *trans*-4,5-dihydroxy-1,2-dithiacyclohexane (DTT_{ox}) (structure **1**; Scheme 1). The photochemically generated geminate radical pair (here, a diradical; structure **2**) will remain in close contact as both radical sites are connected by an aliphatic linker. We will show that photolysis results predominantly in the isomerization to the novel structure **5**, involving an initial pair of thiyl radicals which react via a 1,2- and/or 1,5-H-shift, followed by bond formation between a thiyl and a carbon-centered radical and/or nucleophilic cyclization, respectively. The presence of oxygen does not affect the product yields in the protic solvent water, whereas it does so in the nonprotic solvent dichloromethane (CH_2Cl_2). The latter result suggests a solvent dependence of the H-shift for thiyl radicals, comparable to analogous features of alkoxy radicals ($RO^{\bullet}$).[14]

Experimental Section

Materials. *trans*-4,5-Dihydroxy-1,2-dithiacyclohexane (DTT_{ox}; **1**) was obtained from Sigma-Aldrich Chemical Co. (St. Louis, MO) and used as received. Methylene chloride (CH_2Cl_2) and HPLC-grade acetonitrile (CH_3CN) were purchased from Fisher Scientific (Pittsburgh, PA) and used as received. Water was distilled by a Labconco purification system. D_2O was received from Cambridge Isotope Laboratories, Inc. (Andover, MA), and 3*H*-naphtho[2,1-*b*]pyran-2-carboxylic acid, 10-(2,5-dihydro-2,5-dioxo-1*H*-pyrrol-1-yl)-9-methoxy-3-oxo-, methyl ester (ThioGlo-1) was supplied by Covalent Associates (Woburn, MA).

Photochemical Reactions. Photochemical reactions were carried out either in a Rayonet photoreactor (Southern New England Ultraviolet Company, Branford, CT) or in a custom-built photolysis system. The Rayonet photoreactor was equipped with up to eight RPR-3500 lamps, which emit light between 305 and 410 nm, overlapping with the low-energy part of the UV absorbance of DTT_{ox} (absorbance ca. 250−325 nm; λ_{max} = 280 nm). The custom-built photolysis system was composed of an arc lamp power supply (Model 68806; Oriel Instruments, Stratford, CT), a convective lamp housing (Oriel Instruments) equipped with a 100 W (ozone free) xenon lamp, a monochromator (Model 77250; Oriel Instruments), and an integrating sphere (Labsphere, Inc., North Sutton, NH). The light beam was guided into the monochromator with a fused silica plano convex lens (Oriel Instruments) and from the monochromator into the integrating sphere via a biconvex fused silica lens (Oriel instruments). From the integrating sphere, the reflected light was collected and quantified by a labsphere integrating sphere system control (SC-5500; Labsphere, Inc.). Data acquisition was performed over an RS232 interface using software written in Delphi (Borland, Scotts Valley, CA). The photolysis sample was placed in a specifically adapted quartz cuvette into the integrating sphere, and the monochromator wavelength was set to 297 ± 2 nm (slit width: 280 μm). All samples were prepared in air- or N_2-saturated deionized water or organic solvents of highest commercially available purity. Usually, photolysis times in the Rayonet photoreactor did not exceed 15 min, whereas comparable photolytic yields at a single wavelength in the integrating sphere system required photolysis times of up to 24 h.

Quantum Yields. Quantum yields were determined with the integrating sphere system. To calibrate the integrating sphere system, chemical actinometry was carried out using the ferric oxalate actinometer.[15] A 900 μL aliquot of the actinometry solution was placed in a quartz cuvette that had been modified to fit the integrating sphere. The actinometry solution was irradiated at 297 nm at various times. The reflected light was collected as current by the SC-5500 integrating sphere system control. After irradiation, the solution was vortexed and an 800 μL aliquot of the irradiated solution was transferred to a 10 mL flask. A 4 mL aliquot of 0.2% 1,10-phenanthroline solution and 400 μL of 0.6 M sodium acetate in 1% H_2SO_4 were added. The solution was mixed and allowed to equilibrate for 30 min in the dark at room temperature. After incubation, the absorbance at 510 nm was measured. By knowing the amount of photons

used, a correlation was achieved between the actual current and the photons provided by the light source.

HPLC Analysis. Product separation was carried out on a Hewlett-Packard 1050 instrument equipped with a UV detector. A 100 μL aliquot of diluted sample was injected using an Agilent Technologies 1100 autosampler onto an HPLC column (Phenomenex ODS, 250 × 4.5 mm) and eluted using a linear acetonitrile/trifluoroacetic acid gradient with UV detection at 214 nm. The mobile phase started with 5% mobile phase B [0.1% (v/v) trifluoroacetic acid/90:10% (v/v) acetonitrile/water] at 0 min and increased linearly to 30% mobile phase B within 30 min at a flow rate of 0.8 mL/min. Products were isolated and lyophilized for characterization.

Quantification of H_2O_2. Hydrogen peroxide was measured spectrophotometrically by detecting its titanium sulfate complex at 410 nm, using $\epsilon_{410} = 700$ L mol^{-1} cm^{-1}.[16] Solutions of 1.6×10^{-2} M DTT_{ox} were prepared in water and methylene chloride and irradiated for 10 min using the Rayonet photoreactor equipped with eight RPR-3500 lamps. Aqueous solutions were immediately incubated with titanium sulfate and analyzed by UV spectrophotometry. For the determination of H_2O_2 in CH_2Cl_2, the organic solvent was extracted with water before incubation with titanium sulfate and analysis by UV spectrophotometry.

ESI-Q-TOF MS/MS. Isolated products were lyophilized and reconstituted in 80% methanol containing 5 mM ammonium hydroxide for negative ion electrospray ionization (ESI) MS/MS analysis. The samples were infused directly into the ESI source. ESI-MS/MS spectra were acquired on a Q-TOF-2 (Micromass Ltd. Manchester U.K.) hybrid mass spectrometer operated in the negative MS mode with data acquisition by the time-of-flight (TOF) analyzer. The instrument was operated at isotopic resolution.

NMR Spectroscopy. ^{1}H, COSY (correlation spectroscopy), ^{13}C, and HMQC (heteronuclear multiple-quantum coherence) measurements were performed on a 500 MHz Bruker Avance spectrometer. Isolated products and reagent controls were analyzed in deuterium oxide (D_2O).

FT-IR Spectroscopy. Isolated products were lyophilized and reconstituted with 100 μL of ethanol. Aliquots (10 μL) were placed on disposable polyethylene IR cards, and the solvent was evaporated. The spectra were recorded on a Nicolet Magna-IR 560 instrument using the OMNIC software.

Fluorescence Spectroscopy. Isolated products at a concentration of 3.8 μM were incubated for 30 min with 150 μM ThioGlo-1 at room temperature. In order to quantitate the amount of free thiols labeled with ThioGlo-1, a standard curve of 0−8 μM *N*-Ac-Cys was prepared. The excitation wavelength was 360 nm, and the emission wavelength was 530 nm. Fluorescence yields were measured with a BIO-TEK FL600 microplate fluorescence reader.

Laser Flash Photolysis. The 266 nm excitation source used in the nanosecond flash photolysis experiments was a Quanta-Ray Pro 230 pulsed Nd:YAG laser, operated at 10 Hz. An optical attenuator (variable, Newport Model 935-10) was placed in the laser path in order to reduce the dose delivered to the sample cell to 10−12 mJ/10 ns pulse. The detection system used was similar to one described previously[17] with the following modifications: The present work used a LeCroy LC574A storage oscilloscope (1 GHz). It has a long word length (500 000 points when run as a single channel) that allowed multiple time scales to be saved for each kinetic trace as described elsewhere.[17] The shortest time scale with the LC574A was 0.25 ns/point. One other material difference between the current YAG-based system and that previously reported was the use of a Digikrom 240 monochromator. It, along with the other peripheral instrumentation, is under computer control (PC with a Pentium II processor). The monitor light source was a 1 kW pulsed xenon lamp with an optical path length of 0.5 cm through a rectangular quartz (optically flat) cell. The optical path length of the laser through the sample was 1 cm, and the laser beam was perpendicular to the monitoring beam. The optical cell was part of a gravity-driven flow system.

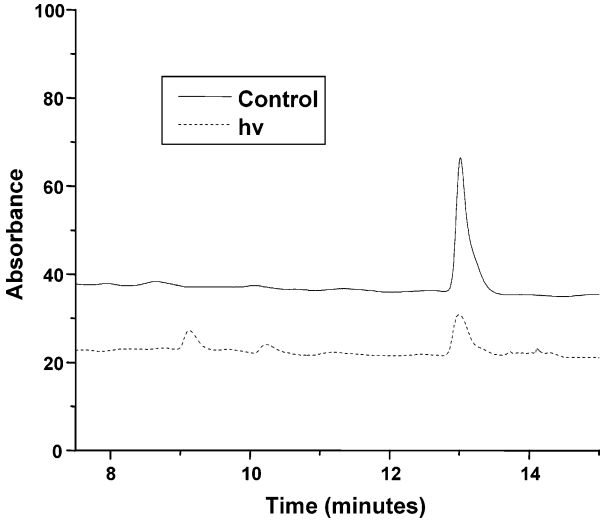

Figure 1. HPLC analyses of control (upper panel) and photolyzed (lower panel) DTT_{ox}. For experimental details, see the Experimental Section.

Results

Product Characterization. Figure 1 shows representative chromatograms, recorded at 214 nm, before and after a 10 min photolysis of 1.6×10^{-2} M DTT_{ox} in air-saturated water. Peaks I and II identify two major reaction products which elute with $t_R = 9.1$ and 10.2 min, respectively. When both products were monitored with a diode array detector, the corresponding UV spectra show an absorbance maximum at $\lambda_{max} \approx 245$ nm with no absorbance at $\lambda > 270$ nm (data not shown).

Products I and II were subjected to negative ion ESI-MS/MS analysis, yielding identical molecular ions $[M-H]^-$ with *m*/*z* 151 (molecular weight of 152). This molecular weight is identical to that of DTT_{ox}, suggesting that I and II are isomerization products. Further evidence that the products are isomers of DTT_{ox} was provided by MS/MS experiments, which yield two dominant fragment ions with *m*/*z* 75 and *m*/*z* 117, corresponding to the loss of CS_2 and the loss of H_2S, respectively. More structural information was gained by H/D exchange experiments. Products I and II were isolated by reversed-phase HPLC, lyophilized, and dissolved into a mixture of D_2O and CD_3OD (8:2, v/v) before negative ion ESI-MS/MS analysis. The resulting molecular ions for both I and II showed $m/z = 153$, indicating three exchangeable protons on each product. The two mass unit increase occurs because loss of a deuteron is expected in the negative ion electron spray process, while the other two exchanged deuterons remain. Consistent with this, the same H/D exchange method shows that for the reactant DTT_{ox}, its two exchangeable protons result in a mass increase of one ($m/z = 152$).

The structures of products I and II were elucidated using ^{1}H, ^{13}C, COSY, and HMQC NMR spectroscopy. As a control, both DTT_{ox} and its reduced, open chain product dithiothreitol (DTT; structure **6** in Scheme 1) were analyzed as well. For DTT, ^{1}H

NMR analysis indicates six nonexchangeable protons. The methylene protons show a chemical shift of 2.6 ppm, whereas the methine protons display a chemical shift of 3.6 ppm. For DTT_{ox}, the methylene protons show a chemical shift of 2.8 and 3.1 ppm, whereas the methine protons are detected at 3.48 ppm. Both control samples, DTT_{ox} and DTT, show no protons with chemical shifts higher than 3.7 ppm.

In product I, five nonexchangeable protons are detected, with three of them showing chemical shifts above 3.7 ppm (Figures S1−S3, Supporting Information). Two signals detected at 2.6 ppm (dd, $J_{vic} = 3.9$ Hz, $J_{gem} = 10.2$ Hz, 1H) and 3.25 ppm (dd, $J_{vic} = 5$ Hz, $J_{gem} = 11.8$ Hz, 1H) likely correspond to a set of two methylene protons. The other three protons are detected with chemical shifts of 3.95 ppm (m, 1H), 4.35 ppm (m, 1H), and 4.6 ppm (d, $J = 4.2$ Hz, 1H).

Product II shows a similar picture with five nonexchangeable protons (Figures S4−S6, Supporting Information). Again, a set of two methylene protons is detected at 2.85 ppm (dd, $J_{vic} = 7.2$ Hz, $J_{gem} = 11.1$ Hz, 1H) and 3.0 ppm (dd, $J_{vic} = 6.2$ Hz, $J_{gem} = 11.1$ Hz, 1H), and the three additional protons have chemical shifts of 3.85 ppm (t, $J = 7.2$ Hz, 1H), 4.08 ppm (m, 1H), and 4.14 ppm (d, $J = 6.7$ Hz, 1H).

The ^{13}C NMR analysis shows four distinct carbon atoms for both product I (detected at 36, 47, 76, and 79 ppm) and product II (33, 46, 76, and 85 ppm).

An HMQC experiment was performed to establish the correlations between the proton and ^{13}C signals. In both products I (Figure S7, Supporting Information) and II (Figure S8, Supporting Information), the protons detected below 3.3 ppm are attached to a carbon in the 30−40 ppm region. Comparison with authentic DTT_{ox} and DTT confirm the presence of one methylene group. In product I, the protons at 3.95 and 4.35 ppm correlate with the carbons at 79 and 76 ppm, respectively. This confirms the presence of two methine protons, both in close proximity to a hydroxyl group. For product II, a similar correlation was observed between the protons at 3.85 and 4.05 ppm and the carbons at 85 and 76 ppm. In both products I and II, the remaining proton correlates with a carbon, which is attached to two sulfur atoms. In order to confirm the connectivities in both products, a COSY experiment was performed, which is displayed in Figure 2. The respective connectivities are summarized in Table 1.

Based on the data provided by negative ion ESI-MS/MS and NMR analysis, we propose that products I and II represent two epimers of 2,3-dihydroxy-1-mercaptotetrahydrothiophene (structure **5**, Scheme 1). The exact stereochemical configurations of the epimers cannot be assigned based on the NMR data.

Further evidence for structure **5** was provided by specific labeling of the free mercapto group with 3*H*-naphtho[2,1-*b*]-pyran-2-carboxylic acid, 10-(2,5-dihydro-2,5-dioxo-1*H*-pyrrol-1-yl)-9-methoxy-3-oxo-, methyl ester (ThioGlo-1). ThioGlo-1 is a maleimide-based label, which fluoresces ($\lambda_{exc} = 379$ nm; $\lambda_{em} = 510$ nm) after Michael addition of a thiol to the maleimide moiety.[18] By comparison to known concentrations of a standard thiol, *N*-acetylcysteine, ThioGlo-1 labeling of products I and II indicates a stoichiometry of one free mercapto group per molecule of I and II (for determinations of the concentrations of I and II, see below: Product Quantification).

We note that the data from MS/MS and ThioGlo-1 labeling also support the thioaldehyde shown in structure **4** (Scheme 1). However, ^{13}C NMR, FTIR and UV−vis spectroscopic analysis show no evidence for the presence of a thioaldehyde: we observed no ^{13}C resonances around 250 ppm, where the thiocarbonyl carbon atom would be expected;[19] FTIR spectroscopic analyses did not show any signal in the 1020−1240 cm^{-1} region, where the >C═S group would absorb.[19,20] When products I and II were monitored with a diode array detector coupled on-line to the HPLC system, we did not detect any significant absorbance around 530 nm, which would be expected for a thioaldehyde.[19]

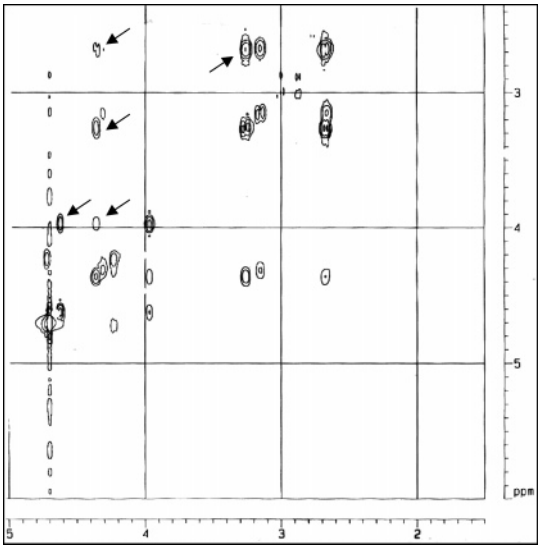

Figure 2. Representative COSY NMR of product I (expanded region). Important connectivities are indicated by the arrows. A summary of the connectivities is given in Table 1. The resonance at ca. 3.15 ppm is caused by a degradation product of I during the time required for recording of the COSY NMR.

TABLE 1: Connectivities of Products I and II as Determined by COSY NMR

product I		product II	
H (ppm)	connectivity	H (ppm)	connectivity
2.6	3.25	2.85	3
	4.35		4.05
3.25	2.6	3	2.65
	4.35		4.05
3.95	4.35	3.85	4.05
	4.6		4.15
4.35	2.6	4.05	2.6
	3.25		3
	3.95		3.85
4.6	3.95	4.15	3.85

Importantly, HPLC (as well as MS/MS and one- and two-dimensional NMR analysis) did not indicate significant yields of any other reaction product besides products I and II immediately after photolysis. However, upon prolonged storage these products I and II proved unstable, with the appearance of degradation products. These degradation products have not been characterized further. We specifically note that the photolysis of DTT_{ox} did not lead to measurable yields of DTT (**6**).

Product Quantification. The response factors for products I and II during HPLC analysis with 214 nm UV detection were determined by ^1H NMR experiments, comparing the absolute yields of protons in products I and II to the quantity of lost protons through consumption of DTT_{ox}. An aqueous (D_2O) solution containing 1.6×10^{-2} M DTT_{ox} and 0.01% (v/v) *tert*-butyl alcohol as an internal standard was prepared as a control sample, and the relative NMR intensities of all protons measured. An air-saturated aqueous (D_2O) solution of 1.6×10^{-2} M DTT_{ox} was photolyzed for 10 min prior to the addition of a final content of 0.01% (v/v) *tert*-butyl alcohol. NMR

measurements were made of all protons from DTT_{ox}, product I, and product II relative to those of the internal standard *tert*-butyl alcohol. The total integrated proton signal lost as a result of DTT_{ox} consumption corresponded quantitatively to that recovered in products I and II. Moreover, the relative distribution of NMR peak intensity between the remaining DTT_{ox} and the products I and II correlated with the relative peak intensities of these products during HPLC analysis. Hence, the response factors of DTT_{ox} and products I and II during HPLC analysis with 214 nm UV detection are identical within experimental error. On the basis of this analysis, the photolysis of **1** generates products I and II at a ratio of 2:1.

Quantum Yields and the Effects of Solvent Nature and Oxygen. By use of an integrating sphere, quantum yields for DTT_{ox} photolysis in water were determined through equations a and b, where P_{abs} is the number of photons absorbed, P_c is the number of photons reflected from a control sample lacking DTT_{ox}, and P_s is the amount of photons reflected from a sample containing DTT_{ox}.

$$\Phi = \text{moles of product/moles of absorbed photons} \quad \text{(a)}$$

$$P_{abs} = P_c - P_s \quad \text{(b)}$$

The moles of product produced were calculated from the peak areas of products I and II recorded during HPLC analysis (vide supra). For air-saturated aqueous solutions, we obtained $\Phi = 1.04 \pm 0.15$ independent of the concentration of DTT_{ox} between 0.33×10^{-3} and 1.6×10^{-2} M. These experiments were performed with the aqueous solution open to air to ensure air saturation during the photolysis. For CH_2Cl_2, such experiments were not feasible because of the evaporation of the solvent during a 24 h photolysis. Therefore, the following comparison between aqueous and CH_2Cl_2 solutions was made based on short periods of irradiation in the Rayonet photoreactor, taking into account a slightly higher absorptivity of DTT_{ox} in CH_2Cl_2 compared to that with H_2O (vide infra):

The photolytic yields of product I and II were independent of oxygen concentration (air- vs N_2-saturated solutions) in water but showed oxygen dependence in CH_2Cl_2. A 10 min light exposure in the Rayonet photoreactor of 1.6×10^{-2} M DTT_{ox} in air-saturated solvent yielded product I at $(7.2 \pm 0.3) \times 10^{-3}$ M in water and $(12 \pm 0.6) \times 10^{-3}$ M in CH_2Cl_2. The relative ratio, $[12 \times 10^{-3}\ \text{M}]/[7.2 \times 10^{-3}\ \text{M}] = 1.7$, of these product yields in CH_2Cl_2 versus H_2O is rationalized by the 1.7-fold higher absorptivity of DTT_{ox} in CH_2Cl_2 compared to that in H_2O in the spectral region overlapping with the emission spectrum of the RPR-3500 lamps. Based on the combined yields of products I and II, we calculate that for 1.6×10^{-2} M DTT_{ox} in CH_2Cl_2, $\Phi = 1.0$. Similarly, a 10 min Rayonet photoreactor exposure of a N_2-saturated aqueous solution of 1.6×10^{-2} M DTT_{ox}, yielded $(7.5 \pm 0.4) \times 10^{-3}$ M of product I indicating no oxygen dependence on the reaction yield in water. In contrast, in N_2-saturated CH_2Cl_2 (1.6×10^{-2} M DTT_{ox}), photolysis yields dropped by about 33% to $(8.0 \pm 0.5) \times 10^{-3}$ M. Based on the combined yields of products I and II in N_2-saturated CH_2Cl_2, we calculate $\Phi = 0.66$.

At lower concentrations of DTT_{ox} (0.33×10^{-2} M), Φ remained equal to 1.0 in water for both air- (vide supra) and N_2-saturated solutions. In CH_2Cl_2, the quantum yield dropped to $\Phi = 0.47$ in air-saturated solution and to $\Phi = 0.07$ in N_2-saturated solution. Thus, the photolytic formation of products I and II is independent of both DTT_{ox} and O_2 concentration in water but highly dependent on both terms in CH_2Cl_2.

Motivated by the oxygen dependence of product formation in CH_2Cl_2, we monitored the photolytic formation of H_2O_2 in this solvent. No H_2O_2 was detected during photolysis of air-saturated solutions of DTT_{ox} in CH_2Cl_2 (<10 μM, based on the LOD from calibration curves).

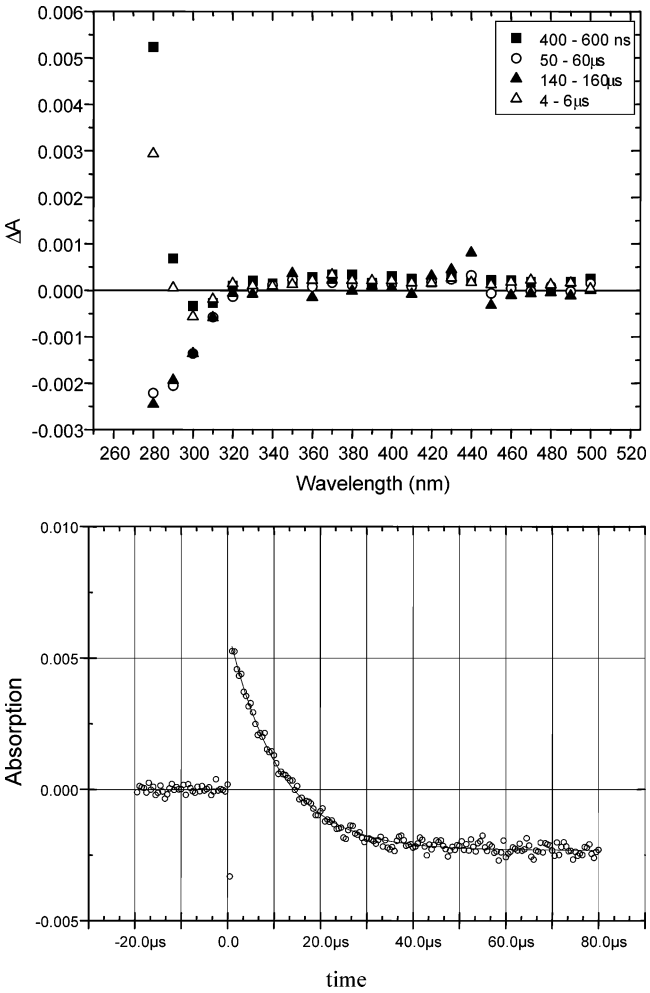

Figure 3. LFP of Ar-saturated aqueous solutions of 1.6×10^{-3} M DTT_{ox} in water. (A) Absorbance spectra recorded within specific periods after the laser flash. (B) Absorption vs time trace recorded at 280 nm. The solid line represents a first-order fit of the experimental data. For experimental details, see the Experimental Section.

Laser Flash Photolysis. Laser flash photolysis (LFP) experiments were performed in order to characterize the primary species generated during DTT_{ox} photolysis. The optical spectra recorded at various time points after 266 nm LFP of 1.6 mM DTT_{ox} in Ar-saturated water and CH_2Cl_2 are displayed in Figures 3A and 4A, respectively. A comparison of both figures reveals some differences between the two solvents, as expected based on the product studies in both solvents presented above. In water (Figure 3A), the spectrum recorded between 400 and 600 ns after the flash is characterized by a strong absorbance at $\lambda < 290$ nm, some photobleaching between 290 and 320 nm, and a weak structureless absorbance between 340 and 460 nm. The absorbance characteristics between 280 and 320 nm likely reflect the superposition of two processes, photobleaching of the ground-state absorbance of DTT_{ox} ($\lambda_{max} = 280$ nm) and formation of a transient Y with $\lambda_{max,Y} < 320$ nm and $\epsilon_{280,Y} > \epsilon_{280,DTTox}$. Optical spectra recorded at longer times after LFP demonstrate that, ultimately, transient Y decomposes into product(s) with lower extinction coefficients at 280 nm compared to those of ground-state DTT_{ox}. This result is consistent with the steady-state photolysis experiments, which show that products I and II have no UV absorbance at $\lambda > 270$ nm (vide supra). Figure 3B shows the respective absorption-versus-time

profile at 280 nm after LFP of DTT_{ox} in Ar-saturated H_2O. Transient Y disappears in a first-order process ($k = 9.1 \times 10^4$ s^{-1}), which ultimately results in photobleaching at this wavelength.

Usually, thiyl radicals show weak absorption bands with $\lambda_{max} = 330$ nm ($\epsilon_{330} < 600$ M^{-1} cm^{-1}, except for penicillamine thiyl radicals) and no significant absorbance between 270 and 300 nm.[21] Hence, it is unlikely that transient Y is a thiyl radical. The spectrum also displays at most minor yields of perthiyl radicals, which are characterized by a distinct strong absorbance with $\lambda_{max} \approx 370$ nm ($\epsilon_{370} \approx 1700$ M^{-1} cm^{-1}).[7,22−24] We can also exclude the formation of significant photolytic yields of disulfide radical anions from DTT_{ox} ($RSSR^{\bullet -}$) which display a strong absorbance band with $\lambda_{max}(RSSR^{\bullet -}) = 390$ nm ($\epsilon_{390} = 6600$ M^{-1} cm^{-1}).[25] At the same time, no radical cations of DTT_{ox} can be observed, which by analogy to several aliphatic disulfides, would absorb with $\lambda_{max}(RSSR^{\bullet +}) \approx 410-440$ nm ($\epsilon \approx 2000$ M^{-1} cm^{-1}).[26] The spectral data in water do not permit the identification of Y. However, by analogy with the spectral characteristics of α-alkylthioalkyl radicals ($R-C^{\bullet}H-S-R'$), which absorb with $\lambda_{max} = 280-290$ nm ($\epsilon \approx 3000$ M^{-1} cm^{-1})[27], the data would be consistent with the intermediacy of an α-mercaptoalkyl radical ($R-C^{\bullet}H-SH$) (vide infra). We do not believe that the observed transient represents the triplet state of the disulfide for the following reason: transient Y decomposes with $k = 9.1 \times 10^4$ s^{-1}. Our steady-state photolysis experiments demonstrate no effect of triplet oxygen on product yields in water. Usually, the reaction of excited triplet states with oxygen proceeds with $k \approx 10^9$ M^{-1} s^{-1}.[28,29] Based on $[O_2] = 2.5 \times 10^{-4}$ M in air-saturated water, we calculate a pseudo-first-order rate constant for the potential reaction of any triplet excited state with oxygen in water of $k \approx 2.5 \times 10^5$ s^{-1}. Therefore, if the 290 nm transient were the triplet excited state, we would have expected significantly lower yields of products I and II in air- versus N_2-saturated solution.

The optical spectrum recorded between 100 and 200 ns after LFP of DTT_{ox} in CH_2Cl_2 (Figure 4A) shows an intense absorbance at $\lambda < 325$ nm, displaying a shoulder at 290 nm. Within 3.5 μs after LFP, this shoulder disappears, leaving an optical spectrum which is characterized by a structureless absorption band increasing toward the UV, and remains rather stable for 160 μs (an absorption-vs-time profile, recorded at 275 nm is shown in Figure 4B). Importantly, also in CH_2Cl_2 no significant yields of perthiyl radicals, disulfide radical anions, and disulfide radical cations are present at any time after the laser flash. Figure 4C shows a difference spectrum obtained by subtraction of the spectrum obtained between 2.5 and 3.5 μs after the pulse from the spectrum obtained between 100 and 200 ns after the pulse. This computation yields a better picture of the 280 nm absorbance, which is immediately present after the laser flash. Again, this 280 nm species could indicate the presence of an α-mercaptoalkyl radical and/or a derivative therefrom (vide infra).

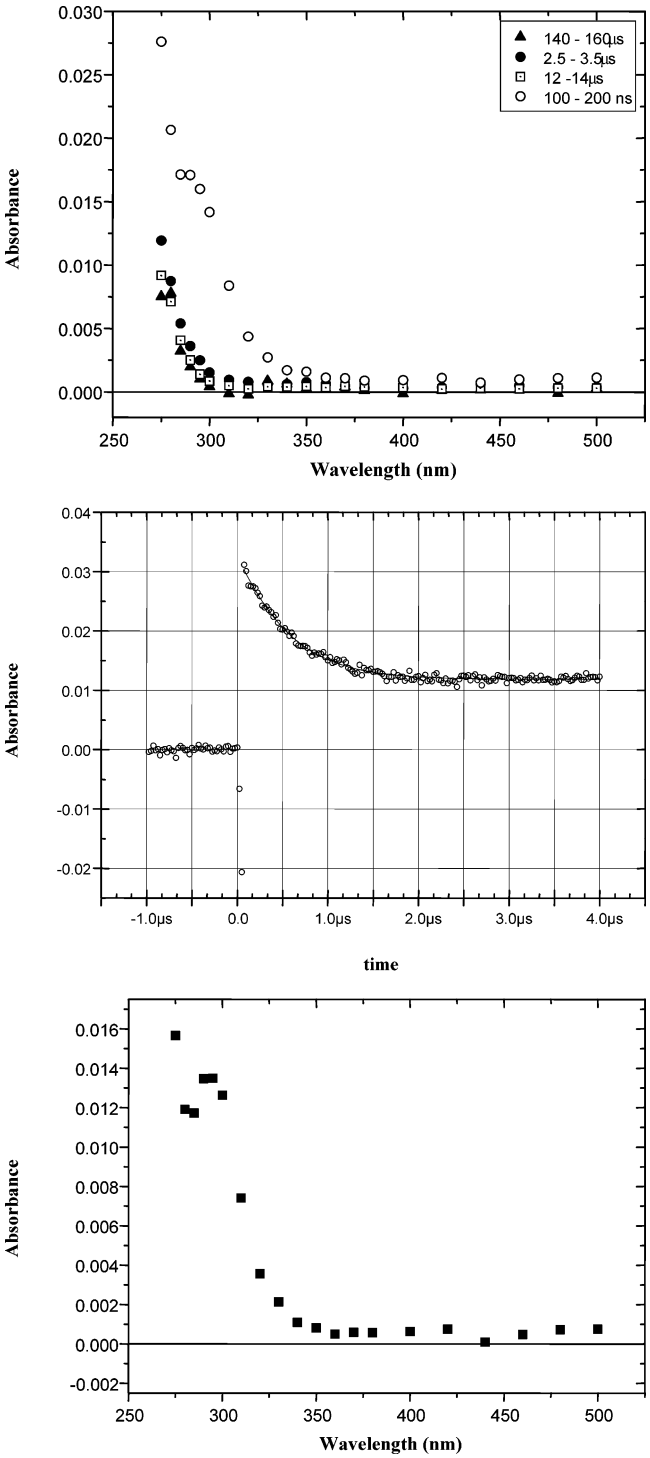

Figure 4. LFP of Ar-saturated solutions of 1.6×10^{-3} M DTT_{ox} in CH_2Cl_2. (A) Absorbance spectra recorded within specific periods after the laser flash. (B) Absorption vs time trace recorded at 275 nm. (C) Difference spectrum computed by subtraction of the spectrum recorded between 2.5 and 3.5 μs from the spectrum recorded between 100 and 200 ns after the laser flash. For experimental details, see the Experimental Section.

Discussion

A mechanistic discussion of our results needs to take into account the following key observations: (i) DTT_{ox} undergoes photoisomerization into two epimeric 2,3-dihydroxy-1-mercaptotetrahydrothiophenes. (ii) Based on LFP experiments, we can discard the intermediacy of perthiyl radicals, disulfide radical cations, and disulfide radical anions. (iii) LFP experiments are consistent with the formation of α-mercaptoalkyl radicals, especially in H_2O. (iv) LFP and steady-state photolysis experiments in CH_2Cl_2 further argue against photoionization of DTT_{ox} as the resulting solvated electrons would react instantaneously with CH_2Cl_2. In this case, only disulfide radical cations would remain as potential precursors for products I and II. (v) There is a 50% higher yield of products I and II upon photolysis of DTT_{ox} in air-saturated compared to N_2-saturated CH_2Cl_2. (vi) There is no difference in product yields between air- and N_2-saturated solutions of DTT_{ox} in H_2O. (vii) No other reaction products are observed in either solvent, with or without oxygen.

SCHEME 2

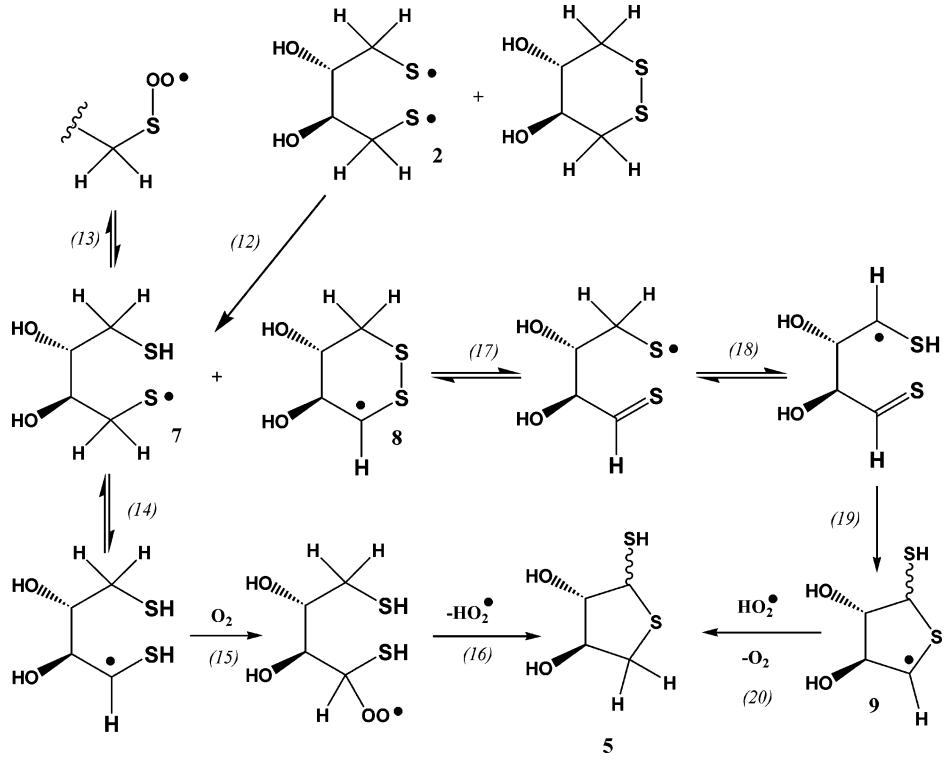

A mechanism accounting for all these observations in H_2O is displayed in Scheme 1. The disulfide bridge of DTT_{ox} in water shows a UV absorbance between 250 and 330 nm with $\lambda_{max} =$ 280 nm. This red shift compared to linear aliphatic disulfides ($\lambda_{max} \approx 250$ nm) is due to significant splitting of the sulfur lone pair orbitals into a higher energy n_- and a lower energy n_+ orbital.[30,31] This splitting is the result of a considerable deviation of the C−S−S−C dihedral angle in the hexacyclic dithiane from 90°, a value generally adopted by sterically unhindered linear aliphatic disulfides. The longer wavelength absorbance of DTT_{ox} is then ascribed to the $n_- \rightarrow \sigma^*$ transition. Our LFP results and product studies suggest that the electron is excited almost exclusively into the σ^* orbital of the S−S bond, resulting in the homolytic cleavage of the S−S bond (reaction 5) (excitation into the σ^* orbital of the C−S bond would lead to homolytic C−S bond cleavage, but perthiyl radicals were not detected by LFP). This is consistent with earlier electron spin resonance (ESR) studies on the photolysis of several cyclic dithianes, including 1,2-dithiacyclohexane, which showed the formation of dithiyl radicals.[32] The resulting diradical could undergo ring closure to regenerate DTT_{ox} (reaction 6); however, in the electronic triplet state such ring closure will be comparatively slow. Two alternative processes will be discussed, both of which will lead to product **5**, a 1,5-H-shift (reaction 7) followed by reaction 9, and a 1,2-H-shift (reaction 10) followed by reaction 11 (it is important to note that, by analogy to alkoxyl radicals,[14] the 1,2-H-shift is likely solvent assisted). Theoretical calculations on H-transfer processes in alkyl radicals[33] show that the 1,5-H-shift is associated with a lower activation barrier compared to the 1,2-H-shift, due to a lower ring strain in the cyclic transition state. In fact, 1,5-H-shifts are synthetically utilized organic reactions of free radicals.[34−36] However, the 1,5-H-shift would yield thiocarbonyl **4**. By analogy to previous examples,[37] the latter is expected to undergo thiophilic addition to regenerate DTT_{ox} (reaction 8). Our results show that product **5** is formed with quantum yields up to 1.0. Hence, if **4** were an intermediate in the formation of **5**, the ring closure of **4** would need to involve a nearly exclusive nucleophilic attack of the mercapto group on the thiocarbonyl carbon (reaction 9). A possible rationale for that could be a kinetic preference of pentacyclization (reaction 9) versus hexacyclization (reaction 8). On the other hand, high quantum yields of **5** would be well explained by a solvent-assisted 1,2-H-shift (reaction 10), followed by carbon−sulfur bond formation (reaction 11). This mechanism would require that $k_{10} \gg k_7$, which is contrary to the theoretical prediction of activation barriers for *intra*molecular H-shifts in ground-state carbon-centered radicals (vide supra).[33] However, such differences in activation barriers may be less pronounced if diradical formation and H-shift proceed in a concerted manner, originating from the excited triplet state (see dashed arrow in Scheme 1). Such a mechanism could also rationalize the rapid formation of a species absorbing with $\lambda_{max} = 290$ nm (potentially the α-mercaptoalkyl radical; vide supra) during LFP, which is observable at times of <1 μs after the laser flash in both solvents, H_2O and CH_2Cl_2. Such rapid formation would not be expected for ground-state thiyl radicals based on pulse radiolysis studies of β-mercaptoethanol: here, a first-order rate constant for the 1,2-H-shift of β-hydroxyalkylthiyl radicals, $HO-CH_2-CH_2-S^{\bullet}$, in H_2O was estimated to $k \approx 2 \times 10^3$ s^{-1}.[9]

For CH_2Cl_2, the mechanism needs to be modified to account for the effects of oxygen and DTT_{ox} concentration. We propose the following reactions, which are displayed in Scheme 2.

There is clear evidence that 1,2-H-shifts of alkoxyl radicals are solvent assisted,[14] catalyzed by solvents which contain hydroxyl groups and have nucleophilic properties. If similar parameters would control 1,2-H-shifts in thiyl radicals, we would expect a considerably less efficient 1,2-H-shift in CH_2Cl_2. As a result, a fraction of diradical **2** may abstract a hydrogen atom from excess substrate in a bimolecular reaction (reaction 12), yielding the monothiyl radical **7** and the carbon-centered radical **8**. The following reactions are hypothetical but are all formulated by analogy to known processes of thiyl radicals and α-mercaptoalkyl radicals.[9] The monothiyl radical **7** could reversibly add oxygen (reaction 13) and reversibly shift the hydrogen (reaction

14). An irreversible exit from these two equilibria would be oxygen addition to the carbon-centered radical (reaction 15), followed by elimination of $HO_2^\bullet$ (reaction 16). However, no dismutation of $HO_2^\bullet$ to H_2O_2 and O_2 appears to be occurring since significant yields of H_2O_2 in CH_2Cl_2 are not detected (vide supra). The carbon-centered radical **8** could potentially undergo ring opening (reaction 17), 1,2-H-shift (reaction 18), ring closure (reaction 19), and ultimate reduction of radical **9** by $HO_2^\bullet$ (reaction 20). The mechanism in Scheme 2 satisfies the observed dependence of photolytic product yields on (i) the presence of oxygen and (ii) the concentration of DTT_{ox} (controlling the rate of reaction 12). Reduction by $HO_2^\bullet$ (reaction 20) is postulated based on the absence of any of its dismutation product, H_2O_2, after photolysis. We note that, theoretically, radical **2** could abstract hydrogen atoms also from the methine carbons of DTT_{ox}[38] which are activated by the α-hydroxy substituents. However, the resulting α-hydroxyalkyl radicals would likely undergo C−S homolysis[38] ultimately generating radicals, which would not be precursors for products I and II. As a consequence, such a mechanism should have generated additional photoproducts, which were experimentally not observed.

Based on the oxygen-dependent increase of the quantum yields of **5** in CH_2Cl_2, we conclude that the 290 nm species formed during LFP in CH_2Cl_2 is most likely not the triplet state. In CH_2Cl_2, the 290 nm species decays into another transient by first-order kinetics with $t_{1/2} = 0.5\ \mu s$, corresponding to $k = 1.4 \times 10^6\ s^{-1}$. Taking a circa 8-times higher solubility of O_2 in organic solvents compared to H_2O, we would expect a pseudo-first-order reaction of the triplet state with O_2 with $k \approx 2 \times 10^6\ s^{-1}$. Hence, the presence of O_2 should cause a measurable decrease of product formation in contrast to our experimental data, which demonstrate that O_2 is a prerequisite for product formation in CH_2Cl_2.

The direct photolytic cleavage of disulfides may play an important role for protein degradation in vivo during the exposure to light, for example, for proteins located in the eye or the skin. In addition, several authors have obtained evidence for both C−S and S−S cleavage of disulfides through interaction with triplet excited states.[39−42] On the basis of these observations, the homolytic cleavage of disulfides does not necessarily require direct exposure to light. For example, triplet excited ketones form during the thermal decomposition of dioxetanes, which are prominent biological oxidation products.[43] These triplet excited states have the potential for direct[44] (via energy transfer) and indirect[45] (via peroxyl radicals) DNA damage and should, in principle, react similarly with proteins.

Conclusion

The photoisomerization of *trans*-4,5-dihydroxy-1,2-dithiacyclohexane (DTT_{ox}) into 2,3-dihydroxy-1-mercaptotetrahydrothiophene **5** is initiated by homolytic cleavage of the disulfide bond. In water, an oxygen-independent mechanism yields **5** via either 1,5- or 1,2-H-shift followed by nucleophilic cyclization or recombination of a sulfur- with a carbon-centered radical, respectively. In the aprotic solvent CH_2Cl_2, a potential mechanism dependent on the concentration of oxygen and DTT_{ox} involves intermolecular H-abstraction and the intermediary formation of oxygen-centered radicals. Products analogous to **5** may represent intermediates to stable covalent aggregates in proteins, especially if the free mercapto group would oxidize further to sulfonic acid. On the basis of the reactions displayed in Schemes 1 and 2 and the solid nature of DTT_{ox}, this disulfide could represent a suitable initiator for controlled free radical reactions in the solid state. In fact, our preliminary data show that thiyl radicals of DTT_{ox} oxidize added mercaptanes in the solid state.

Acknowledgment. We are grateful to Pfizer, Inc. and NIH CA072987 for financial support. The work described herein was also supported by the Office of Basic Energy Sciences of the U. S. Department of Energy. This paper is Document No. NDRL-4485 from the Notre Dame Radiation Laboratory.

Supporting Information Available: ^1H NMR spectra (Figures S1−S6) and HMQC spectra (Figures S7 and S8) of products I and II. This material is available free of charge via the Internet at http://pubs.acs.org.

References and Notes

(1) Creighton, T. E. *Proteins*; W. H. Freeman and Company: New York, 1993.
(2) Nicolaou, K. C.; Dai, W.-M. *Angew. Chem., Int. Ed. Engl.* **1991**, *30*, 1387−1416.
(3) Nicolaou, K. C.; Smith, A. L. *Acc. Chem. Res.* **1992**, *25*, 497−503.
(4) Greer, A. *J. Am. Chem. Soc.* **2001**, *123*, 10379−10386.
(5) Brzostowska, E. M.; Greer, A. *J. Am. Chem. Soc.* **2003**, *125*, 396−404.
(6) Boyd, D. B. *J. Am. Chem. Soc.* **1972**, *94*, 8799−8804.
(7) Morine, G.; Kuntz, R. R. *Photochem. Photobiol.* **1981**, *33*, 1−5.
(8) Grant, D. W.; Stewart, J. H. *Photochem. Photobiol.* **1984**, *40*, 285−290.
(9) Zhang, X.; Zhang, N.; Schuchmann, H.-P.; von Sonntag, C. *J. Phys. Chem.* **1994**, *98*, 6541−6547.
(10) Scheffer, J. R. In *Organic Solid State Chemistry*; Desiraju, G. R., Ed.; Elsevier: Amsterdam, 1987; pp 1−45.
(11) McBride, J. M. *Acc. Chem. Res.* **1983**, *16*, 304−312.
(12) Byrn, S. R.; Pfeiffer, R. R.; Stowell, J. G. *Solid-State Chemistry of Drugs*; SSCI, Inc.: West Lafayette, IN, 1999.
(13) Feng, X. W.; McBride, J. M. *J. Am. Chem. Soc.* **1990**, *112*, 6151−6152.
(14) Konya, K. G.; Paul, T.; Lin, S.; Lusztyk, J.; Ingold, K. U. *J. Am. Chem. Soc.* **2000**, *122*, 7518−7527.
(15) Murov, S. L.; Carmichael, I.; Hug, G. L. *Handbook of Photochemistry*, 2nd ed.; Marcel Dekker: New York, 1993.
(16) Eisenberg, G. M. *Ind. Eng. Chem. Anal. Ed.* **1943**, *15*, 327−328.
(17) Thomas, M. D.; Hug, G. L. *Comput. Chem. (Oxford)* **1998**, *22*, 491−498
(18) Wright, S. K.; Viola, R. E. *Anal. Biochem.* **1998**, *265*, 8−14.
(19) Ando, W.; Ohtaki, T.; Suzuki, T.; Kabe, Y. *J. Am. Chem. Soc.* **1991**, *113*, 7782−7784.
(20) Silverstein, R. M.; Webster, F. X. *Spectrometric Identification of Organic Compounds*, 6th ed.; John Wiley & Sons: New York, 1998.
(21) Hoffman, M. Z.; Hayon, E. *J. Phys. Chem.* **1973**, *77*, 990−996.
(22) Elliot, A. J.; McEachern, R. J.; Armstrong, D. A. *J. Phys. Chem.* **1981**, *85*, 68−75.
(23) Burkey, T. J.; Hawari, J. A.; Lossing, F. P.; Lusztyk, J.; Sutcliffe, R.; Griller, D. *J. Org. Chem.* **1985**, *50*, 4966−4967.
(24) Everett, S. A.; Schöneich, Ch.; Stewart, J. H.; Asmus, K.-D. *J. Phys. Chem.* **1992**, *96*, 306−314.
(25) Von Sonntag, C. In *Sulfur-Centered Reactive Intermediates in Chemistry and Biology*; Chatgilialoglu, C., Asmus, K.-D., Eds.; NATO ASI Series, Series A: Life Sciences; Plenum Press: New York, 1990; Vol. 197, pp 359−366.
(26) Bonifacic, M.; Schäfer, K.; Möckel, H.; Asmus, K.-D. *J. Phys. Chem.* **1975**, *79*, 1496−1502.
(27) Hiller, K.-O.; Asmus, K.-D. *Int. J. Radiat. Biol.* **1981**, *40*, 597−604.
(28) Gijzeman, O. L. J.; Kaufman, F.; Porter, G. *J. Chem. Soc., Faraday Trans. 2* **1972**, *69*, 708−720.
(29) Turro, N. J. *Modern Molecular Photochemistry*; The Benjamin/Cummings Publishing Co., Inc.: Menlo Park, CA, 1978; pp 589−590.
(30) Kosower, N. S.; Kosower, E. M. In *Free Radicals in Biology*; Pryor, W. A., Ed.; Academic Press: New York, 1976; Vol. II, pp 55−84.
(31) Creed, D. A. *Photochem. Photobiol.* **1984**, *39*, 577−583.
(32) Smissman, E. E.; Sorenson, J. R. J. *J. Org. Chem.* **1965**, *30*, 4008−4010.
(33) Viskolcz, B.; Lendvay, G.; Körtvélysi, T.; Seres, L. *J. Am. Chem. Soc.* **1996**, *118*, 3006−3009.

(34) Barton, D. H. R.; Beaton, J. M.; Geller, L. E.; Pechet, M. M. *J. Am. Chem. Soc.* **1960**, *82*, 2640−2641.
(35) Lopez, J. C.; Alonso, R.; Fraser-Reid, B. *J. Am. Chem. Soc.* **1989**, *111*, 6471−6473.
(36) Dorigo, A. E.; McCarrick, M. A.; Loncharich, R. J.; Houk, K. N. *J. Am. Chem. Soc.* **1990**, *112*, 7508−7514.
(37) Viola, H.; Hartenhauer, H.; Mayer, R. *Z. Chem.* **1988**, *28*, 269−277.
(38) Akhlaq, M. S.; von Sonntag, C. *J. Am. Chem. Soc.* **1986**, *108*, 3542−3544.
(39) Walling, C.; Rabinowitz, R. *J. Am. Chem. Soc*. **1959**, *81*, 1137−1143.
(40) Byers, G. W.; Gruen, H.; Giles, H. G.; Schott, H. N.; Kampmeier, J. A. *J. Am. Chem. Soc.* **1972**, *94*, 1016−1018.
(41) Rosenfeld, S. M.; Lawler, R. G.; Ward, H. R. *J. Am. Chem. Soc*. **1972**, *94*, 9255−9256.
(42) Gruen, H.; Schott, H. N.; Byers, G. W.; Giles, H. G.; Kampmeier, J. A. *Tetrahedron Lett.* **1972**, *37*, 3925−3928.
(43) Cilento, G.; Adam, W. *Free Radical Biol. Med.* **1995**, *19*, 103−114.
(44) Epe, B.; Muller, E.; Adam, W.; Saha-Möller, C. R. *Chem.-Biol. Interact*. **1992**, *85*, 265−281.
(45) Adam, W.; Arnold, M. A.; Saha-Möller, C. R. *J. Org. Chem.* **2001**, *66*, 597−604.